ISSN 1070-3632, Russian Journal of General Chemistry, 2015, Vol. 85, No. 5, pp. 1005–1018. © Pleiades Publishing, Ltd., 2015.
Original Russian Text © G.I. Kobzev, Yu.V. Zaika, 2015, published in Zhurnal Obshchei Khimii, 2015, Vol. 85, No. 5, pp. 705–719.

Peculiarities of Formation of Hydroxonium Ion and Its Small Clusters

G. I. Kobzev and Yu. V. Zaika

Orenburg State University, pr. Pobedy 13, Orenburg, 460018 Russia
e-mail: zaika.jylia@mail.ru

Received October 16, 2014

Abstract—Density functional theory combined with the restricted open-shell Hartree–Fock method using the B3LYP, BLYP, and B3PW91 exchange-correlation functionals in the 6-311G** basis has been applied to determine equilibrium geometry of water-containing clusters $^1(H_3O^+–nH_2O)$ with n = 1–3, 5, 6 and $^1(H_3O^+–3H_2O)Cl^–$. The SA-MCSCF simulation has revealed a series of electronic terms of hydroxonium ion and energy profiles of its formation. Energy profiles of H_3O^+ interaction with H_2O have been simulated and analyzed. Vibrational spectra have been simulated for all the mentioned complexes in the equilibrium state, and regularities of changes of the fundamental vibrational frequencies with the increasing nuclearity of the complexes have been discovered.

Keywords: hydroxonium ion, aquatic complex, vibrational spectrum, potential energy surface, DFT, ROHF

DOI: 10.1134/S1070363215050011

Microstructure of the upper atmosphere is known for its diversity and determines a number of macroscopic atmospheric processes. For instance, smaller constituents of air (clusters of water molecules with hydroxonium ion as well as certain inorganic and organic molecules) participate in formation of aerosols that enter the lower atmosphere via mass transfer and turbulent diffusion and enhance formation of clouds, thunderstorms, typhoons, hurricanes, and tornados [1]. Acting as catalyst, hydroxonium ion determines the rate of aerosols formation and the composition of related oxidation reactions.

Besides the above-mentioned phenomena, a number of reactions occur in the low-temperature plasma at the height above 100 km, involving cations [O^+, O_2^+, O_4^+, H^+, H_2^+, OH^+, HO_2^+, H_2O^+, (O_2^+–H_2O), H_3O^+, (H_3O^+–H_2O), (H_3O^+–$2H_2O$), and (H_3O^+–OH)], anions ($O^–$, $O_2^–$, $O_3^–$, $H^–$, and $OH^–$), neutral atoms (O and H [2]) and molecules (H_2, O_2, and H_2O, their intermolecular interactions removing restrictions on deactivation or singlet oxygen generation [3–5]; O_3), free radicals (OH and HO_2 yielding excited oxygen and H_2O_2 molecules [6] via recombination), exited atoms {$O(^1D_1)$ [7], $O(^1S_0)$}, and excited singlet oxygen O_2 ($^1\Delta_g$) [8–10]. Furthermore, the H_3O^+–$n(H_2O)$ (n = 1–9) small clusters existing in the gas phase may distort the radio signals. In view of the above, study of electronic and spectral properties of such objects is important for resolving fundamental issues related to catalytic reactions in plasma and practical safety issues of aviation and space flights.

Experimental and theoretical studies of structure, photochemical, and physico-chemical properties of various water clusters have been addressed in a number of contributions [11–19]. In particular, it has been demonstrated that the binding energy per water molecule increases from 27 kJ/mol in the $(H_2O)_2$ dimer to 35–40 kJ/mol in the $(H_2O)_5$ and $(H_2O)_6$ clusters, remaining constant in the larger clusters [17–19].

Geometry of hydroxonium ion clusters with several (up to 10) water molecules in gas and condensed phase has been studied in detail as well [20–30]. However, selectivity of the intermolecular bonding involving hydroxonium ion and its effect on the cluster nuclearity have remained the open issues so far. Furthermore, the reported lengths of hydrogen bonds and OH groups in the mentioned clusters have been uncertain; potential energy surfaces of hydroxonium ion formation and decomposition have not been analyzed; assignments of vibrations of O–H bond of

hydroxonium ion and the protonated $H^+(H_2O)_n$ (n = 5–8) systems to the vibrational frequencies have been ambiguous [24]; IR spectroscopy data for hydroxonium ion has been contradictory [26–38].

This work aimed to elucidate the features of hydroxonium ion interaction with water molecules, to analyze the possibility of hydroxonium ion formation (from ground as well as excited states of the fragments) and decay, and to reveal the changes of vibrational frequencies as well as charge and spin parameters of H_3O^+ with the increasing nuclearity of its small aqueous clusters.

Study of structure and reactivity of water clusters with hydroxonium ion and chlorine atom will aid in resolving certain ecological problems, since these clusters may participate in the processes affecting the local weather changes at industrial districts where chlorine is among other pollutants. Furthermore, particles of sea salt containing chlorine are constant components of coastal and oceanic air [40].

Optimization of natural geometry parameters of H_2O molecules, H_3O^+ ions, and H_3O^+–nH_2O (n = 1–3, 5, and 6) complexes was performed using the density functional theory (DFT) in the frame of the restricted Hartree-Fock method [41] with B3LYP, BLYP, and B3PW91 exchange-correlation potentials in the 6-311G** basis as implemented in GAMESS [42] software package. Vibrational and electronic spectra were simulated using the B3LYP functional and the 6-311G** basis allowing the best coincidence between the experimental and the simulated O–H dissociation energy and geometry parameters of H_2O molecule [18, 25–28]. On top of that, the B3LYP and B3PW91 functionals could adequately reproduce vibrational frequencies of the H_3O^+ ion and its clusters with water molecules [15, 16, 23, 31–35]. Cross-sections of potential energy surfaces of formation and decomposition of H_3O^+ ion and H_3O neutral molecule ($H^+ + H_2O \leftrightarrow H_3O^+$, $H + H_2O^+ \leftrightarrow H_3O^+$, $H + H_2O \leftrightarrow H_3O$) were obtained in the frame of the SA-MCSCF method via averaging over the first 20 states in the active space of 14 electrons at the 20 MO (14, 20).

Structure of hydroxonium ion in the gas phase and cross-sections of potential energy surface of its formation. To date, two models of formation of H_3O^+ and $H_5O_2^+$ ions have been mainly considered. The Eigen model assumes addition of a proton to an isolated water molecule to form the H_3O^+ ion (known as hydroxonium ion). The second structure described by the Zundel model is an ion of water dimer with a proton equally belonging to the both parent molecules. In the Eigen structure, the excessive charge of hydrated proton is delocalized between the three hydrogen atoms, whereas the Zundel structure contains the excessive charge localized at a single hydrogen atom located between the water molecules. The O–H bond lengths and bond angles in the H_3O^+, H_2O, and $H_5O_2^+$ particles simulated via quantum-chemical methods using different basis functions [16, 18, 20, 21, 25, 27–29, 33, 35, 36] as well as these determined from vibrational and NMR spectral data are significantly discrepant (Table 1).

The O–H bond lengths determined in this work for the isolated hydroxonium ion and water molecule differed by no more than 0.01–0.03 Å, and the difference between the H–O–H bond angles in those particles was of 8.2°–15.7° depending on the functional used. The O–H bond length in the $H_5O_2^+$ complex was somewhat longer, of 1.190–1.210 Å depending on the simulation method and basis (Table 1).

The optimized parameters of equilibrium states of the Zundel [25, 30] and Eigen [21, 30] hydroxonium ions, water molecule [18, 25–28], and the H_3O^+–$n(H_2O)$ (n = 2, 3) complexes [18, 23, 29, 30] obtained by us using the DFT method with different functionals (Tables 1 and 2) coincided with the results of spectral [16, 42], resonance, and X-ray diffraction measurements as well as with the simulation data [16, 18–20, 25, 27–29, 33, 35, 36].

The O–H bond in the H_3O^+ ion (the Eigen model) was strong [d_e(O–H) 5.29 eV] (see figure), similarly to the O–H bond in the H_2O molecule [d_e(O–H) = 5.12 eV] [18].

Cross-sections of potential energy surfaces of the $H + H_2O^+ \leftrightarrow H_3O^+$, $H^+ + H_2O \leftrightarrow H_3O^+$, and $H^0 + H_2O^0 \leftrightarrow H_3O^0$ reactions are shown in the figure.

As expected, the ground state term of the H_3O^0 neutral system was dissociative (figure, curve *1*). A special interest should be given to the term of the corresponding excited doublet state (figure, curve *2*) (S = 0.5) $^2H_3O^{0*}(\uparrow)$ located in the close neighborhood of the ground state term and dissociating following the $^2H_3O^{0*}(\uparrow) - {}^2[{}^3H_2O^*(\uparrow\uparrow) + {}^2H^0(\downarrow)]$ scheme. The minimum of the latter term is located at R = 1.2±0.05 Å. The well depth in the minimum point was of d_e = 2.20 eV. Probably, this excited state acts as a highly reactive short-living intermediate in fast

Table 1. Geometry parameters of H_2O molecule, H_3O^+ and $O_2H_5^+$ ions, and $(H_3O^+–3H_2O)Cl^–$ cluster

Geometry parameter	H_2O	H_3O^+	$O_2H_5^+$	$(H_3O^+–3H_2O)Cl^–$
R(O–H) $_{H_2O,\ H_3O^+}$, Å	0.962[a], 0.972[b], 0.959[c], 0.950–0.959 [18, 25–27]	0.979[a], 0.989[b], 0.977[c], 0.969–0.982 [25, 30]	0.968[a], 0.978[b], 0.966[c], 0.958–0.970 [21, 25]	0.960, 0.983, 1.014[a] 0.972, 1.008, 1.047[b] 0.961, 0.994, 1.032[c]
R[O(H_3O^+) – O(H_2O)], Å	–	–	2.400[a], 2.430[b], 2.393[c], 2.385–2.415 [20, 21]	2.843[a], 2.570[b], 2.531[c]
∠HOH $_{H_2O,\ H_3O^+}$, deg	103.9[a], 103.1[b], 103.9[c], 103.8–104.3 [18, 26, 28]	112.3[a], 111.5[b], 112.0[c], 112.5–120.0 [25, 30]	109.3[a], 108.4[b], 109.1[c], 109.4–110.1 [21, 25]	103.8, 104.4[a] 104.6, 102.6[b] 103.1, 105.3[c]
∠[O(H_3O^+)H(H_3O^+)O(H_2O)], deg	–	–	174.1[a], 173.5[b], 174.1[c], 174.6 [21]	161.9[a], 166.4[b], 166.3[c]

[a] ROB3LYP. [b] ROBLYP. [c] ROB3PW91, data from this work.

processes involving H_2O and H_2O^+ under conditions of ionizing irradiation in the upper atmosphere.

The simulation (see figure) revealed that collision of the H_2O^+ ion with the H atom resulted in a barrier-free formation of the $(H_3O)^+$ ground state (see figure, curve *3*) (D_e 5.29 eV) with low electron affinity (E = 1.07). Such term behavior was due to the structure change coming from the pseudo crossing of energy terms (curves *3* and *7*). In view of that, we concluded that the barrier-free formation of hydroxonium ion occured via the $[^1H_2O^0(\uparrow\downarrow) + H^+] – {}^1H_3O^+(\uparrow\downarrow)$ scheme, the cross-section of the potential energy surface corresponding to the $[^2H_2O^+(\uparrow) + {}^2H^0(\downarrow)]$ reaction remaining dissociative. In the course of decomposition of hydroxonium ion (curve *3*), the proton drained the electron density and eliminated as a hydrogen atom at the dissociation limit.

Hence, the equilibrium ground state of hydroxonium ion was fairly stable in the gas phase in the absence of free electrons; however, the $H_3O^+ + e = H_3O^*$ reaction was equivalent to the transition between the terms of the H_3O^+ state (figure, curve *3*) and the equilibrium excited state H_3O^* (curve *2*), the latter could either decompose into the H_2O^* and H particles or be deactivated via transition into the term of the ground state of the H_3O neutral molecule (curve *1*) followed by dissociation into H_2O and H. In the both cases, the process should be accompanied by the energy release. Let us recall that an electron addition to the H_3O^+ ion to yield H_3O followed by the $H_3O^+ + e = H_3O^* \rightarrow H_3O \rightarrow H_2O + H$ dissociation (necessarily involving the H_3O^* excited state and accompanied by the energy release) is among the major redox processes in the upper atmosphere.

Noteworthily, the dissociative limit of the cross-section of the $^1H_3O^+$ potential energy surface characterizing the reaction of water molecule with a proton $\{[^1H_2O^0 + H^+] \leftrightarrow {}^1H_3O^+(\uparrow\downarrow)\}$, (figure, curve *7*) was located at the area of higher energy than those of curves *3–6* describing the reactions involving the H_2O^+ ion. Therefore, decomposition of hydroxonium ion without the electron trapping should follow the $[^1H_2O^0 + H^+] \leftrightarrow {}^1H_3O^+(\uparrow\downarrow) \rightarrow H_2O^+(\uparrow) + H(\downarrow)$ scheme, as mentioned above.

Table 2. Geometry parameters of H_3O^+–$2H_2O$, H_3O^+–$3H_2O$, H_3O^+–$5H_2O$, and H_3O^+–$6H_2O$ clusters

Geometry parameter	H_3O^+–$2H_2O$	H_3O^+–$3H_2O$	H_3O^+–$5H_2O$	H_3O^+–$6H_2O$
$R(O–H)_{H_2O}$, Å	0.964[a], 0.974[b], 0.962[c], 0.949–0.968 [23, 29]	0.964[a], 0.974[b], 0.962[c], 0.948 [29]	0.962–1.002[a], 0.972–0.998[b], 0.959–0.983[c]	0.962–0.997[a], 0.974–1.013[b], 0.971–0.981[c]
$R(O–H)_{H_3O^+}$, Å	0.966–1.045[a], 0.976–1.061[b], 0.964–1.048[c], 0.965–0.969 [23], 1.038–1.047 [23]	1.015[a], 1.030[b], 1.016[c], 0.983–1.016 [22, 29, 30]	0.963–1.148[a], 0.973–1.175[b], 0.961–1.161[c]	1.023[a], 1.036[b], 1.023[c]
$R[O(H_2O) – H(H_3O^+)]$, Å	1.449[a], 1.464[b], 1.434[c], 1.435–1.453 [23]	1.546[a], 1.554[b], 1.533[c], 1.533–1.549 [30]	1.258–1.464[a], 1.258–1.473[b], 1.235–1.456[c]	1.549[a], 1.576[b], 1.549[c]
$R(O_1–O_2)$, Å	2.491[a], 2.513[b], 2.479[c], 2.509 [29]	2.559[a], 2.582[b], 2.547[c], 2.560–2.580 [22, 29]	2.405–2.501[a], 2.431–2.524[b], 2.395–2.492[c]	2.557[a], 2.593[b], 2.556[c]
$\angle(H_1OH_2)_{H_2O}$, deg	107.4[a], 106.5[b], 107.2[c], 106.8–106.9 [23]	106.5[a], 105.7[b], 106.4[c], 108.0 [29]	107.6–109.0[a], 105.6–108.3[b], 104.8–106.6[b], 107.5–109.1[c]	107.2[a], 106.8[b], 107.3[c]
$\angle(H_1OH_2)_{H_3O^+}$, deg	111.2–115.3[a], 110.1–114.0[b], 111.0–115.4[c], 112.1–114.1 [23]	112.0–112.2[a], 110.9–111.0[b], 111.7–112.0[c], 114.4–115.0 [30]	109.0–115.2[a], 107.9–114.4[b], 108.7–115.4[c]	106.2–106.3[a], 105.5–105.6[b], 106.2–106.3[c]
$\angle[O(H_3O^+)H(H_3O^+)O(H_2O)]$, deg	174.6[a], 174.1[b], 174.7[c], 174.3–176.3 [17]	175.2[a], 174.6[b], 175.3[c]	175.4–175.6[a], 174.0–175.1[b], 175.7–175.5[c]	174.3[a], 166.1[b], 167.3[c]
$\angle[H(H_3O^+)O(1H_2O)H(1H_2O)]$, deg	122.8[a], 120.0[b], 120.3[c], 125.5–127.3 [23]	118.1–121.8[a], 115.7–118.9[b], 117.7–121.1[c]	114.6–115.7[a], 111.9–115.8[b], 114.7–114.8[c]	106.7–126.6[a], 101.8–115.4[b], 101.7–116.0[c]
$\angle[H(H_3O^+)O(2H_2O)H(2H_2O)]$, deg	119.0[a], 119.6[b], 119.7[c], 121.0–123.4 [23]	118.1–121.8[a], 115.7–118.9[b], 117.8–121.4[c]	116.4–119.0[a], 113.8–118.7[b], 116.0–118.9[c]	105.3–127.4[a], 101.9–115.4[b], 101.7–115.9[c]
$\angle[H(H_3O^+)O(3H_2O)H(3H_2O)]$, deg	–	118.2–121.7[a], 119.0–115.8[b], 117.7–121.2[c]	–	104.7–127.2[a], 101.8–115.5[b], 101.7–115.8[c]

[a] ROB3LYP. [b] ROBLYP. [c] ROB3PW91, data from this work.

In view of the above, irradiation of water with the protons beam should result in generation of atomic and/or molecular hydrogen and in water ionization (the H_2O^+ ions formation), whereas electron trapping with hydroxonium ion should be accompanied by energy release. The conclusion has been supported by the data reported in [44] demonstrating that the protons interaction with water differs depending on the protons velocity. Note that intersection of curves *7* and *10* in the figure caused by the spin-orbital interaction can yield the short-living metastable excited state of the $^3H_3O^{+*}(\uparrow\uparrow)$ ion, further decomposing to form H_2O^+.

Structure and hygroscopicity of small clusters of hydroxonium ion with water. The available data has led to conclusion that interaction of hydroxonium ion with water molecules results in formation of intermolecular complexes, their stability being determined by the strongest hydrogen bond between the hydrogen atom and the oxygen atom of water molecule. The strongest O–H hydrogen bond was formed in the $H_5O_2^+$ complex (Table 3).

The individual $H_5O_2^+$ ion showing the specific electronic, geometry, and spectral parameters (Table 1) could exclusively exist in the gas phase at very low pressure and temperature: according to the performed simulation, any contact of the mentioned ion with one or several water molecules led to its transformation into the intermolecular complex (cluster) nH_2O, n = 1–6 (Tables 1 and 2) with the altered properties. Hence, the $H_5O_2^+$–$n(H_2O)$ clusters should yield the H_3O^+–$(n+1)(H_2O)$ ones, in agreement with the data of Jiang et al. [24].

Hydroxonium ion H_3O^+ formed an unsymmetrical system with two water molecules (Table 2). Each of the water molecules of the formed structure was connected with a hydrogen atom of the hydroxonium ion via a single hydrogen bond, $R[O(H_3O^+) – O(H_2O)]$ = 2.491±0.004 Å. The O–H bonds of the hydroxonium ion participating in the hydrogen bonding were extended to 1.045 Å at the average, whereas the third O–H bond became shorter, of 0.966 Å (Table 2). Such complexes were observed in the atmosphere at the height of above 100 km as well as in the ionosphere; under those conditions, the complexes could interact with metal ions and further participate in catalytic processes of aerosols formation. Similar trends were observed in the case of the complex of hydroxonium ion with five water molecules (Table 2).

The H_3O^+–$3H_2O$ complex was a regular pyramid with the hydroxonium ion located in its vertex. The base of the pyramid consisted of three water molecules. Oxygen atoms of water molecules were located in the vertexes of the equilateral triangle, ∠OOO ≈ 60° and $R(O–O)_{H_2O}$ = 4.269±0.01 Å. The lateral edge of the pyramid was of $R[O(H_3O^+) – O(H_2O)]$ = 2.559 Å, the angles at the pyramid vertex being practically equal (112.05°) (Table 2). Those results coincided well with the earlier reported data [16, 24, 29, 30].

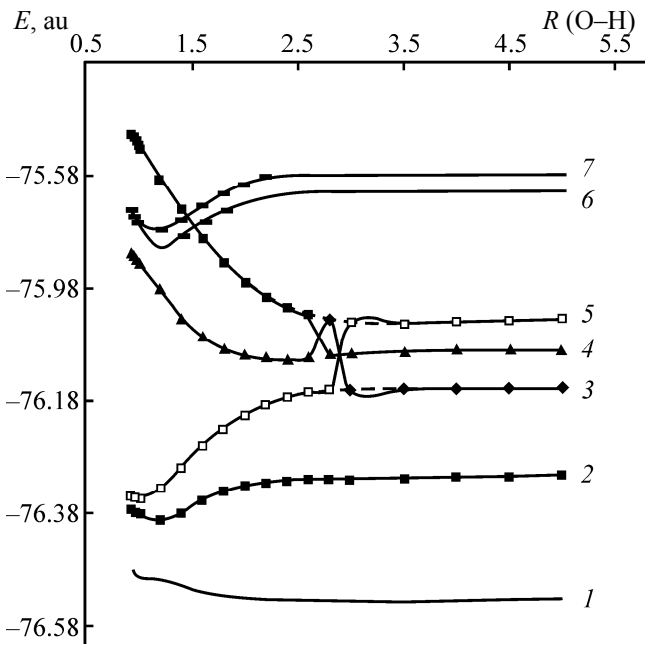

Cross-sections of energy surface of electronic terms of hydroxonium ion formation. See notation for *1*–*7* in the text.

The complex of hydroxonium ion with six water molecules could be viewed as a symmetrical pyramid with the H_3O^+ ion in its vertex (Table 2). Each of the hydrogen atoms of the hydroxonium ion was connected with one water molecule via a hydrogen bond {$R[O(H_3O^+) – O(H_2O)]$ = 1.549 Å}, and oxygen atoms of the three water molecules nearest to the hydroxonium ion formed an isosceles triangle ΔOOO with R(O–O) = 3.825±0.005 Å and the [$O(H_2O)$–

Table 3. Separation energy of water molecules in $2(H_2O)$ dimer and molecular complexes of hydroxonium ion with water molecules

Complex	E_b, eV	Complex	E_b, eV
$H_5O_2^+$	1.39	$H_2O–H_2O$	0.28
H_3O^+–$2H_2O$	1.25	H_3O^+–$3H_2O$	0.95
H_3O^+–$5H_2O$	0.61	$3H_2O–H_3O^+–H_2O$	0.089

$O(H_3O^+)$– $O(H_2O)$] angle at the vertex of 97°±0.1°. The rest three water molecules were also symmetrically located around the central oxygen atom of the H_3O^+ ion with the $\angle O(H_2O)O(H_3O^+)O(H_2O)$ angle being of 80.5±0°. The edges of that isosceles triangle were 4705±0.005 Å long. The length of the hydrogen bond O–H between the nearest water molecule and the hydroxonium atom in the H_3O^+–$6H_2O$ complex was of 1.55 Å, somewhat shorter than that in water dimer R(O–H) = 2.004 Å according to the simulation].

Hence, the O–H bond length in the symmetrical complexes of hydroxonium ion with three and six water molecules was marginally changed with the complex nuclearity (1.015–1.023 Å), and the bond angles decreased from 112.2° to 106.3°, the lowest values being observed for the $(H_3O^+–3H_2O)Cl^–$ system (Table 1).

The length of the O–H bond forming the hydrogen bonding between hydroxonium ion and water molecules increased with increasing the number of water molecules in hydrate shell of the H_3O^+ ion (Table 1).

Increase of the O–H bond length was the most prominent in the case of the complex with chloride ion $(H_3O^+–3H_2O)Cl^–$ (by 0.03 Å). The obtained values were in good accordance with the data reported earlier for the similar systems [45].

It has been earlier qualitatively considered that propensity of the H_3O^+ ion to form hydrogen bonds should be significantly higher and its O–H bonds should be somewhat longer as compared to the corresponding parameters of water molecules. The ∠HOH angle in the OH_3^+ ion should be higher than that in water molecule (104°31'), however remaining below the tetrahedral one (109°28') [16].

Indeed, our simulation revealed that strength of the O–H hydrogen bonds between hydrogen atom of the hydroxonium ion and oxygen atom of the water molecule in the $(H_3O)^+$–$n(H_2O)$ (n = 1–6) clusters decreased with the increased nuclearity of the cluster, remaining higher than that in the H_2O–H_2O dimer (Table 3). That evidenced about the higher hygroscopicity of small clusters of hydroxonium ion with water molecules $(H_3O)^+$–$n(H_2O)$ (n < 10) as compared with that of water clusters $n(H_2O)$.

To conclude, hygroscopicity of the $(H_3O)^+$–$n(H_2O)$ clusters decreased with increasing number of the water molecules (n); simultaneously the O–H bonds of water molecules and the cation participating in the hydrogen bonding became shorter, the O–O distances between the adjacent water molecules in the first shell decreased with more of the water molecules in the second shell; the H–O–H angles in the water molecules forming the hydration shell of the hydroxonium ion ranged in between 105.35° and 109.0°; the angles between the O–H bonds of the hydroxonium ion in the symmetrical complexes steadily decreased.

Stereospecificity of intermolecular interactions between hydroxonium ion and water molecules in the small clusters. It is generally accepted that oxygen atom of a hydroxonium ion forms four equivalent hybrid orbitals (sp^3 hybridization) with three of them belonging to the covalent bonds and the forth being populated with a pair of non-bonding electrons (lone-electron pair). In this instance, electronic structure of hydroxonium ion is similar to that of ammonia molecule.

According to the structural data on molecular orbitals (MO) of the H_3O^+ ion (Tables 4 and 5) and the NH_3 molecule, all the molecular orbitals had the similar structure, with the highest occupied molecular orbital (HOMO) being majorly determined by the contribution from $2p_z$ atomic orbital (AO) with certain admixture of $2s$(O) and $1s(H_{1,2,3})$ AOs. The lone-electron pair of ammonia is known to participate in the ammonium ion formation ($NH_3 + H^+ = NH_4^+$); however, the OH_4^+ ion cannot be formed, and existence of the unstable H_4O^{2+} particle is questionable [46].

It was therefore of interest to investigate stereospecificity of formation of the O–H hydrogen bonds by hydroxonium ion in the course of its hydration. The O···H hydrogen bond in the H_3O^+–$(H_2O)_n$ clusters should grow stronger with the enhanced polarization of the charge density (high in the absolute value and of the opposite signs) at the O and H atoms of the different molecules participating in the hydrogen bonding. Comparison of the charges at atoms obtained via the different simulation methods revealed that the charge at the oxygen atom of H_3O^+ ranged in between +0.047 and –0.029 e, even its lowest value being below that at the oxygen atom in water molecule (–0.5 e) (Table 4), whereas the charges at the hydrogen atoms of H_3O^+ were more positive than those at the hydrogen atoms of H_2O.

It could be presumed that H_3O^+ ions were capable of strong hydrogen bonding with oxygen atoms of H_2O molecules (the hydrogen bond being stronger than that in water dimer) and weaker hydrogen bonding between H_3O^+ oxygen and H_2O hydrogen atoms.

Table 4. Electronic properties of H_3O^+ ion[a]

Property	MNDO/d	MINDO/3	AM1	PM3	DFT/B3LYP/RHF/6-311G (2p,2d)
E_{total}, kcal/mol	–8235.8	–8017.1	–8150.4	–7633.7	–48148.8
E_b, kcal/mol	–81.7	–70.6	–72.4	–56.8	–122.0
E, kcal A^{-1} mol^{-1}	1×10^{-4}	6×10^{-7}	6×10^{-5}	9×10^{-7}	4×10^{-3}
μ, D	1.415	2.175	2.340	1.925	1.623
q, e	0.886	1.600	1.645	1.247	1.000
no. Z at.	Charges				
4 8 O	–0.029	–0.199	–0.108	0.047	–0.135
3 1 H	0.343	0.400	0.369	0.318	0.378
2 1 H	0.343	0.400	0.369	0.318	0.378
1 1 H	0.343	0.400	0.369	0.318	0.378
R(O–H), Å	0.964	0.966	1.004	0.978	0.978
α(HOH), deg	115.3	109.6	107.8	109.4	112.3

[a] Charges at atoms of water molecule simulated via those methods were of: q(O) –0.50 e and q(H) +0.25 e.

Indeed, the simulation revealed asymmetry of hydrogen bonds in the H_3O^+–$4H_2O$ cluster. Analysis of cross-sections of potential energy surface pointed at formation of only three strong hydrogen bonds between hydrogen atoms of the hydroxonium ion and oxygen atoms of water molecules (Table 3). As expected, the weakest hydrogen bond was formed via coordination of the H_2O molecule at the oxygen atom in the vertex of trigonal pyramid of the hydroxonium ion. Strength of the weakest hydrogen bond decreased with the increasing nuclearity of the cluster. For instance, the well depth in the potential energy cross-section was the smallest (0.04 eV) in the case of hydroxonium ion complex with six water molecules. That evidenced about expulsion of the hydroxonium ion out of the water cluster of any nuclearity, due to the stronger hydrogen bong in the water dimer H_2O–H_2O as compared with the O–H_2O bond at the vertex of the H_3O^+ pyramid.

IR spectra of water molecule, hydroxonium ion, and its clusters with water. Hydroxonium ions H_3O^+ can be found in the form of thermally unstable particles in the gas phase, in the form of hydrated hydrogen ions in water and aqueous acids (even though their lifetimes are very short, $T_{1/2} = 10^{-13}$ s), in the form of H_3O^+ trigonal pyramid with the H–O–H bond angle of ≈115° in crystalline acids, and in certain minerals and artificial inorganic compounds. In some complex minerals the presence of hydroxonium ion has been suggested theoretically; certain crystal hydrates contain associates of hydroxonium ions with water molecules [16]. Thermally unstable, the H_3O^+ ions decompose with elimination of water in the gas phase, for instance, upon heating of the acidic form of zeolite in vacuum.

Earlier reports have marked formation of H_3O^+ and their role in redox processes in the Earth atmosphere [1], in the molecular adsorption of water at oxides surface (in certain cases, for example, for dehydroxylated alumina [47], the dissociative adsorption of water yielding surface hydroxyl group being the preceding stage), in biological systems (for example, biological action of ionizing radiation leading to the local acidification of the aqueous system along the charged particle track caused by hydroxonium ion rather than water radiolysis products: OH, H, O_2^-, or H_2O_2 [48]).

Despite a number of experimental studies having confirmed the presence of H_3O^+ particles, hydroxonium ion has remained scarcely studied so far. In particular, there have been much less of spectrochemical and theoretical studies of hydroxonium ion as compared to similar reports on other hydroxyl compounds and water. Infrared spectroscopy has been recognized as a powerful method to determine the presence of water, hydroxyl groups, and hydroxonium

Table 5. Symmetry and energy of molecular orbitals of H_3O^+ ion[a]

MO number	1	2	3	4, HOMO	5, LUMO	6	7
Symmetry	1A1	1E	1E	2A1	3A1	2E	2E
Energy, eV	–41.06	–27.49	–7.49	–23.91	–6.63	–3.99	–3.99
AO *Z* no.	Charges						
s O 4	0.87349	–0.00000	0.00000	0.26735	–0.40686	–0.00000	0.00000
p_x O 4	0.00270	0.31487	0.76678	0.01916	–0.00680	0.53372	0.16622
p_y O 4	–0.00560	–0.76597	0.31532	–0.03978	0.01411	0.16657	–0.53320
p_z O 4	–0.13143	0.03912	0.00230	–0.93322	0.33106	0.00386	0.02614
s H 2	0.27062	0.38518	–0.24506	0.13624	0.49147	0.31194	–0.60079
s H 3	0.27062	0.01964	0.45610	0.13624	0.49147	–0.67627	0.03025
s H 1	0.27062	–0.40481	–0.21104	0.13624	0.49147	0.36433	0.57054

[a] Structures of MO of H_3O^+ ion and NH_3 molecule as simulates via different methods were qualitatively the same.

ion in liquid, gaseous, and crystalline hydroxyl-containing compounds; however, the studies have revealed different absorption bands in the spectrum of H_3O^+ [16]. Being fairly broad, these bands have not been accurately located. On top of that, the bands assigned to hydroxonium ion overlap with these of water molecules, giving rise to continuous adsorption at 900–1800 cm^{-1}, further complicating experimental study of hydroxonium ion complexes with water.

The early studies have aimed to estimate parameters of hydroxonium ion in the gas phase reasoning from the similarity between electronic structures of water and the H_3O^+ ion. It has been assumed that the O–H bond should be about 0.99–1.0 Å long, since the length of the corresponding bonds of free and bound water is of 0.96–0.98 Å. Hence, the presence of associates of hydroxonium ion with water molecules has been suggested for the compounds with O–H bonds longer than 0.98 Å.

According to the IR spectroscopy data, the band of degenerate deformation vibration of the H_3O^+ ion was stronger than that of the symmetric deformation vibration. Furthermore, the former band was narrower than the stretching bands; the stretching bands were somewhat stronger but more diffuse, strongly overlapped, and could not be easily identified in the spectrum.

Comparison of IR spectra of water molecule and hydroxonium ion revealed that positions of the ν(OH) stretching bands were not characteristic for identify-cation of hydroxonium ion structure. The band of doubly degenerate deformation vibration seemed the only characteristic signal pointing at the presence of hydroxonium ion [16]. For instance, a band at 1650 cm^{-1} assigned to deformational vibrations of H_3O^+ as well as other deformational bands of H_3O^+ at 1120 and 1150 cm^{-1} have been observed in the spectra of mica, phlogopite, and muscovite as well as optical crystals of hexagonal lithium periodate [49].

It has been concluded that a broad strong IR absorption band in the spectra of hydrated titanium dioxide $TiO_2 \cdot H_2O$ with maxima at 3800–2600 cm^{-1} is due to the presence of the free terminal OH groups and the groups participating in hydrogen bonding, whereas the low ν(OH) values (2851–2592 cm^{-1}) have been attributed to the presence of hydroxonium ion in the structure [50]. Since it is generally assumed that the δ(HOH) deformational vibrations of the H_3O^+ ion are manifested at 1670–1800 cm^{-1}, a group of the bands with maximums at 1696 and 1685 cm^{-1} has been considered characteristic of hydroxonium ion in the $TiO_2 \cdot H_2O$ structure [50].

In the case of perchloric acid hydrate $HClO_4 \cdot H_2O$, the bands assigned to deformational vibrations of the

H_3O^+ ion have been observed at 1670 and 2820–2400 cm^{-1}. The spectrum of the $HClO_4 \cdot 2H_2O$ hydrate contains deformational δ(HOH) vibration bands of the $H_5O_2^+$ ion at 1680 cm^{-1} [51]. Similarly, deformational vibrations give rise to the bands at 2780 and 1680 cm^{-1} in the case of $HNO_3 \cdot H_2O$ [52] and at 1700 cm^{-1} in the case of hydrated liquid SO_2 [53]. The mentioned bands as well as low-frequency ν(OH) bands below 2900 cm^{-1} have been assigned to O–H vibrations of the H_3O^+ ion; however, its characteristic bands are found in a different spectral range [54, 55].

Fundamental frequencies of hydroxonium ion (ν_1 = 3370, ν_2 = 938, ν_3 = 3575, and ν_4 = 1670 cm^{-1}) have been determined theoretically using the transition equations [56] as well as via the Hartree–Fock method implemented in GAUSSIAN-98 software package (in the 3-21G or 6-311G basis accounting for the scaling factors of 0.9085 and 0.9051 as recommended in Ref. [57]). The quantum-chemical simulation performed in [56] has not allowed for unambiguous prediction of vibrational spectrum of hydroxonium ion, leading to significant deviations from the known values: ν_1 = 3490 [54] and 3760 cm^{-1} [55], ν_2 = 960 [54] and 1050 cm^{-1} [55], ν_3 = 3610 [54] and 3870 cm^{-1} [55], and ν_4 = 1590 [54] and 1550 cm^{-1} [55]. The accuracy of the bands positions found in Ref [54] has been claimed as of below 200 × 10^2 m^{-1} (ν_1, ν_3, and ν_4) and below 100 × 10^2 m^{-1} (ν_2).

Analysis of results of simulation of IR spectra of H_2O, H_3O^+, and H_3O^+–$(H_2O)_n$ clusters taking into account the animation structure allows for confident assignment of the bands to stretching, deformational, and librational vibrations of the listed particles. Comparison of the spectra concludes about shifting of the maximums, changing the bands width, and appearance of new peaks with increasing the cluster nuclearity and evolution of its structure.

The simulated spectrum of H_2O contained a pair of weak single bands corresponding to the symmetric 3778 cm^{-1} (3652–3857 cm^{-1} [16, 33]) and asymmetric 3935 cm^{-1} (3756–3913 cm^{-1} [16, 18]) stretching along with a stronger deformational band at 1650 cm^{-1} (1595–1650 cm^{-1} [16, 18]) and a translational band.

In contrast to the IR spectrum of H_2O, that of the H_3O^+ ion contained three lines making up a strong broad band in the region of stretching vibrations, two of the lines corresponding to asymmetric vibrations, at 3607 and 3706 cm^{-1} (3518–3560 cm^{-1} [28, 36]) and a weaker one at 3535 cm^{-1} being assigned to symmetric stretching (3389–3491 cm^{-1} [27]). Two degenerate deformational vibrations were observed at 1677 and 1687 cm^{-1} (1625 and 1638 cm^{-1} [37]), whereas symmetric deformational (umbrella) band was found at 891 cm^{-1} (954 cm^{-1} [39]). Detailed information of the simulated fundamental vibrational frequencies in IR spectra of water molecule, hydroxonium ion, and their associates (1 to 6 water molecules) is collected in Table 6. The determined parameters well coincided with theoretical data and experimental spectroscopy studies [16, 18, 27–29, 32–37], thus indirectly confirming validity of the performed simulations.

Let us analyze evolution of characteristic bands of H_3O^+ and H_2O upon formation of their small clusters and increasing the clusters nuclearity.

Characteristic frequencies of the isolated H_3O^+ ion were as follows: $\nu_{as}(OH)(H_3O^+)$ = 3607 and 3706 cm^{-1} (3518–3560 cm^{-1} [28, 36]), $\nu_s(OH)(H_3O^+)$ = 3535 cm^{-1} (3389–3491 cm^{-1} [27]), $\delta_{as}(HOH)(H_3O^+)$ = 1677 and 1687 cm^{-1} (1625 and 1638 cm^{-1} [37]), and $\delta_s(HOH)(H_3O^+)$ (umbrella) 891 cm^{-1} (954 cm^{-1} [39]) (Table 6). All stretching bands of H_3O^+ revealed the red shift by 150–200 cm^{-1}, and the deformational bands showed the blue shift by 30–50 cm^{-1} as compared with IR spectrum of water.

Appearance of the isolated $H_5O_2^+$ particles resulted in the combination bands absent in the IR spectra of water and hydroxonium ions, cm^{-1}: $\delta(HOH)(H_2O)$ + $\nu(OH)(H_2O)$ = 1756(21) + 1707(0.014); $\nu(OH)(H_2O)$ + $\delta(HOH)$ H_2O = 1554(2.6) + 1468(6.7); $\nu_{as}(OH)(H_2O)$ 3825 $(H_2O)(1)$, 3815 $(H_2O)(2)$; $\nu_s(OH)(H_2O)$ 3731 $(H_2O)(1)$, 3744 $(H_2O)(2)$; $\nu(OH)(H_2O)$ 975(26) (proton transfer between the H_2O molecules). Two of the combination vibration maximums possessed the blue shift, and the other two vibrations revealed the red shift as compared with the simulated deformational frequencies of water molecule (1650 cm^{-1}) and hydroxonium ion (1677 and 1687 cm^{-1}). Frequencies of asymmetric and symmetric stretching of $H_5O_2^+$ were lower than those of water (ν_{as} = 3935 and ν_s = 3778 cm^{-1}) but higher than those of hydroxonium ion (ν_{as} = 3607 and 3706 cm^{-1}, ν_s = 3535 cm^{-1}). On top of that, IR spectrum of isolated $H_5O_2^+$ particles contained a maximum at $\nu(OH)(H_2O)$ 975(26) cm^{-1} corresponding to a proton transfer between the H_2O molecules. Frequency of that maximum was somewhat higher than the δ_{umbr} = 891 cm^{-1} (954 cm^{-1} [39]) of the sym-metric (umbrella) deformational vibration of the H_3O^+ ion.

Table 6. Theoretical and experimental vibrational frequencies (ν, cm^{-1}) of H_2O molecule, H_3O^+ ion, and $^1(H_5O_2^+)$, $^1(H_3O^+–2H_2O)$, $^1(H_3O^+–3H_2O)$, $^1(H_3O^+–5H_2O)$, $^1(H_3O^+–6H_2O)$, and $(H_3O^+–3H_2O)Cl^–$ complexes

Vibration type	H_2O	H_3O^+	$O_2H_5^+$	$H_3O^+–2H_2O$	$H_3O^+–3H_2O$	$H_3O^+–5H_2O$	$H_3O^+–6H_2O$	$(H_3O^+– 3H_2O)Cl^–$
ν_s	3778, 3657 [18], 3857 [16], 3770 [33], 3652 [33]	3535, 3535 [36], 3491 [27], 3490 [28], 3389 [27]	3744, 3731, 3617 [28], 3608 [29]	3804 (H_2O) (I), 3791 (H_2O) (II), 2564 (H_3O^+), 3639 (H_2O) [35], 3604 (H_2O) [35], 2509 (H_3O^+) [35]	3804 (H_2O) (I), 3785 (H_2O) (II), 3756 (H_2O) (III), 2966 (H_3O^+), 3644 (H_2O) [35], 3612 (H_2O) [35], 2874–2931 (H_3O^+) [22, 35]	2697 (H_2O) (I), 3374 (H_2O) (II), 3494 (H_2O) (III), 3778 (H_2O) (IV), 3799 (H_2O) (V), 2588 (H_3O^+)	3774 (H_2O) (I), 3664 (H_2O) (II), 3637 (H_2O) (III), 3285 (H_2O) (IV, VI), 3242 (H_2O) (V, VI), 3171 (H_2O) (IV, V), 2977 (H_3O^+)	3370 (H_2O) (I), 3301 (H_2O) (II), 2823 (H_3O^+)
δ	1650, 1650 [16], 1595 [18], 1595 [33], 1548 [33]	1677, 1687, 1638 [37], 1626 [37]	1756, 1707, 1756 [34], 1741 [32]	1619 (H_2O) (I), 1638 (H_2O) (II), 1697 (H_3O^+), 1720 (H_3O^+)	1668 (H_2O) (I), 1650 (H_2O) (II), 1636 (H_2O) (III), 1742 (H_3O^+), 1729 (H_3O^+), 1583 [34]	1599 (H_2O) (I), 1644 (H_2O) (II), 1655 (H_2O) (III), 1682 (H_2O) (IV), 1692 (H_2O) (V), 1733 (H_3O^+), 1773 (H_3O^+)	1686 (H_2O) (I), 1684 (H_2O) (II), 1677 (H_2O) (III), 1649 (H_2O) (IV), 1639 (H_2O) (V), 1636 (H_2O) (VI), 1805 (H_3O^+), 1802 (H_3O^+)	1670 (H_2O) (I), 1663 (H_2O) (II), 1662 (H_2O) (III), 1795 (H_3O^+), 1790 (H_3O^+)
ν_{umbr}	–	891, 954 [39]	–	1282	1271	1516	1442	1529
ν_{as}	3935, 3756 [18], 3913 [16], 3798 [33], 3756 [33]	3607, 3706, 3560 [28], 3550 [28], 3519 [36]	3826, 3815, 3693 [28, 29], 3662 [28, 29]	3898 (H_2O) (I), 3878 (H_2O) (II), 3718 (H_2O) [35], 3724 (H_2O) [35], 2337 (H_3O^+), 3775 (H_3O^+), 2381 (H_3O^+) [35], 3626 (H_3O^+) [35], 3580 (H_3O^+) [35]	3915 (H_2O) (I), 3906 (H_2O) (II), 3864 (H_2O) (III), 3725 (H_2O) [35], 2805 (H_3O^+), 2753 (H_3O^+), 2804 (H_3O^+) [35]	3857 (H_2O) (I), 3875 (H_2O) (II), 3919 (H_2O) (III), 3940 (H_2O) (IV), 3943 (H_2O) (V), 3961 (H_3O^+)	4002 (H_2O) (I), 3957 (H_2O) (II), 3954 (H_2O) (III), 3914 (H_2O) (IV), 3852(H_2O) (V), 3815 (H_2O) (VI), 2741 (H_3O^+), 2661 (H_3O^+)	3976 (H_2O) (I), 3957 (H_2O) (II), 3829 (H_2O) (III), 3283 (HCl), 3283 (H_3O^+), 2504 (H_3O^+)

IR spectrum of the $H_3O^+–2H_2O$ complex contained a diffuse band at 3775–3897 cm^{-1} caused by symmetric and asymmetric vibrations of two water molecules. The band position was almost the same as the range of the corresponding band in the water spectrum, but its intensity was lower. The medium-intensity band at $\nu(OH)(H_3O^+)$ = 3775(4.5) cm^{-1} corresponding to a large-amplitude (0.65–1.50 Å) asymmetric vibration of the only free O–H bond of the H_3O^+ ion could be hardly identified without the amination representation due to overlap with the $\nu_s(H_2O)$ = 3778 cm^{-1} band.

The spectrum of the H_3O^+–$2H_2O$ cluster contained a strong band absent in IR spectra of H_2O, H_3O^+, and $H_5O_2^+$. The first maximum of that band was assigned to asymmetric stretching of hydroxonium ion 2337(94.6) cm^{-1} with one of the O–H bonds of H_3O^+ participating in the hydrogen bonding was extended and the other similar bond was shortened; the terminal O–H (H_3O^+) bond was inactive in the vibration. The second maximum was assigned to a symmetric stretching of hydroxonium ion 2564(28.4) cm^{-1} with the both O–H bonds participating in the hydrogen bonding extending and shortening synchronously. The presence of those bands $\nu_{as}(OH)$ = 2337(94.6) and $\nu_s(OH)$ = 2564(28.4) cm^{-1} in IR spectrum of H_3O^+–$2H_2O$ could be considered characteristic of the presence of H_3O^+ particle in the discussed system.

Deformational vibrations of hydroxonium ion [1697(0.7) and 1720(0.7) cm^{-1}] and of water [1619(0.6) and 1637(0.3) cm^{-1}] were always mutually combined, complicating their assignment without considering the animation.

A medium-intensity band $\delta(HOH)H_3O^+$ with maximum at 1282(5.3) cm^{-1} in IR spectrum of the H_3O^+–$2H_2O$ complex was also a characteristic one, pointing at the presence of hydroxonium ion in the complex. It revealed a blue shift as compared with an umbrella band of H_3O^+ (891 cm^{-1}).

Similarly to the other above-discussed IR spectra, that of H_3O^+–$3H_2O$ contained the ν(OH) bands with maximums at 3915(3), 3906(3), and 3864(3) cm^{-1} (asymmetric stretching of H_2O), at 3804(1.2), 3785 (1.4), and 3756(1.2) cm^{-1} (symmetric stretching of H_2O), and at 2966–2753 cm^{-1} (similar to the band at $\nu_{as}(OH)(H_3O^+)$ = 2337(94.6) and $\nu_s(OH)(H_3O^+)$ = 2564(28.4) cm^{-1} in IR spectrum of the H_3O^+–$2H_2O$ complex).

The peak at 2966(11.1) cm^{-1} in IR spectrum of H_3O^+–$3H_2O$ corresponded to symmetric stretching of H_3O^+ with large amplitude of vibration of all the three hydrogen atoms. The strongest IR peak at 2753(70.3) cm^{-1} reflected asymmetric stretching in H_3O^+. The both peaks revealed the blue shift as compared to the corresponding bands in the H_3O^+–$2H_2O$ spectrum. Noteworthily, the third stretching maximum at 2805(62.5) cm^{-1} was observed in the H_3O^+–$3H_2O$ spectrum, assigned to the ν(OH) vibration with abnormally high amplitude (0.44–1.56 Å) of one of the three hydrogen atoms of hydroxonium ion. That could be rationalized as proton transfer from the H_3O^+ ion to the hydrogen-bonded water molecule. That vibration revealed a small contribution from symmetric stretching of the bound water. All those three strong maximums could serve as characteristic signals of hydroxonium ion presence in the H_3O^+–$3H_2O$ complex, in contrast to the weak deformation bands in hydroxonium ion [1742(0.3) and 1729(0.4) cm^{-1}] and in water molecule [1668(0.4), 1650(1.3) and 1636(1.4) cm^{-1}].

Another characteristic band pointing at the presence of the H_3O^+ ion in the H_3O^+–$3H_2O$ cluster was a medium-intensity peak at 1271(5.7) cm^{-1}; similarly to the case of the H_3O^+–$2H_2O$ complex, it was shifted towards high-frequency range as compared to the corresponding band of isolated hydroxonium ion (891 cm^{-1}).

Similarly to the spectra of complexes of lower nuclearity, IR spectrum of the H_3O^+–$5H_2O$ complex (with one of the O–H bonds of hydroxonium ion remaining free) contained a weak diffuse band at 3700–4000 cm^{-1} consisting of a set of asymmetric and symmetric vibration bands of H_2O molecules not involved in the hydrogen bonding. In particular, the band contained a peak with maximum at 3961(2.8) cm^{-1} assigned to the stretching of terminal O–H group of the H_3O^+ cation. That vibration with large amplitude (0.46–1.5 Å) of the only hydrogen atom not involved in the hydrogen bonding could be considered as a vibration describing the proton elimination. However, that vibration could not be used as a characteristic signal of the presence of hydroxonium ion in the H_3O^+–$5H_2O$ complex without the vibration animation analysis. Noteworthily, the symmetrical vibrations of the two water molecules with only a single OH group participating in the hydrogen bonding shifted towards lower frequency range [3494(21.5) and 3374(21.8) cm^{-1}] (Table 6). The both peaks assigned to symmetrical vibrations of water molecules in IR spectrum of the H_3O^+–$5H_2O$ clusters were fairly strong, pointing at a variety of hydrogen bonding types in the complex.

Furthermore, IR spectrum of the H_3O^+–$5H_2O$ cluster contained a band at 2500–2750 cm^{-1} revealing two strong maximums. They corresponded to symmetrical [2588(60.5) cm^{-1}] and asymmetrical [2696(42.5) cm^{-1}] $\nu(OH)(H_3O^+)$ stretching. The presence of that band in IR spectrum is a characteristic signal of the presence of H_3O^+ ion in the structure.

The 1500–1800 cm^{-1} band in the spectrum of the same cluster contained eight maximums corresponding to combination deformational bands of hydroxonium ion and water molecule as well as to those of various

water molecules. Only in the cases of four high-frequency maximums the contribution from the $\delta(H_3O^+)$ vibration was higher than that of water deformational vibration: 1773(13.3) = $\delta(H_3O^+)$ + $2\delta(H_2O)$ + $\nu(OH)(H_3O^+)$; 1733(0.08) = $\delta(H_3O^+)$ + $2\delta(H_2O)$ + $\nu(OH)(H_3O^+)$; 1696(1.2) = $\delta(H_3O^+)$ + $3\delta(H_2O)$; 1681(2.7) = $2\delta(H_3O^+)$ + $\delta(H_2O)$.

All those maximums revealed the blue shift by 20–100 cm^{-1} with respect to the similar vibrations of water and hydroxonium ion; however, the most high-frequency peak was the strongest one, and could therefore serve as a signal of the presence of H_3O^+ ion in the complex.

A broad band at 800–1200 cm^{-1} in the H_3O^+–$5H_2O$ cluster spectrum consisted of a set of combination deformational bands of hydroxonium ion and water molecules as well: $\delta(H_3O^+)$ + $\delta(H_2O)$ + $\nu(OH)(H_3O^+)$ + $\nu(OH)(H_2O)$. The maximums at 852(4.0) and 831(2.6) cm^{-1} corresponded to torsion and deformational bands of water: $\nu_{tors}(H_2O)$ + $\delta(H_2O)$. A weak band at 701(0.6) cm^{-1} was a combination torsion vibration of water molecule and hydroxonium ion: $\nu_{tors}(H_3O^+)$ + $2\nu_{tors}(H_2O)$.

The maximum at 1515(6.3) cm^{-1} in the same spectrum was assigned to a combination H_3O^+ umbrella and torsion water vibrations: $\delta_{umbr}(H_3O^+)$ + $2\nu_{tors}(H_2O)$. That maximum was similar to the corresponding peaks in the H_3O^+, H_3O^+–$2H_2O$, and H_3O^+–$3H_2O$ spectra, characteristic of the presence of the H_3O^+ ion in the complexes; but in the case of the H_3O^+–$5H_2O$ cluster that signal was shifted towards high-frequency domain.

Two strong maximums at 2741(40.3) and 2661(40.1) cm^{-1} in IR spectrum of the H_3O^+–$6H_2O$ complex corresponded to asymmetric stretching of hydroxonium ion, whereas a maximum at 2977(19.4) cm^{-1} was assigned to the symmetric stretching of H_3O^+. The strongest maximum of umbrella deformation at 1442(7.9) cm^{-1}, a part of a weak band at 1400–1800 cm^{-1}, could serve as confirmation of hydroxonium ion presence in that complex.

Hence, the increasing number of water molecules in the H_3O^+–nH_2O complex resulted in appearance of a group of the maximums at 1400–1500 cm^{-1} and 1700–1800 cm^{-1} assigned to the $\delta(HOH)$ = $\delta(HOH)(H_3O^+)$ + $\delta(HOH)(H_2O)$ (medium) and $\delta(HOH)$ = $\delta(HOH)(H_2O)$ + $\delta(HOH)(H_3O^+)$ (weak) combination bands, correspondingly, on top of the overlapping maximums at 1550–1650 cm^{-1} [$\delta(HOH)(H_3O^+)$ and $\delta(HOH)(H_2O)$]. Frequency and intensity of the combination bands with the higher $\delta(HOH)(H_3O^+)$ contribution grew higher with the increasing cluster nuclearity; therefore, those bands could be considered a signal pointing at the presence of the H_3O^+ ions in the system.

Another characteristic indication of the presence of the H_3O^+ ion in the H_3O^+–nH_2O complex ($n \rightarrow 1$) was a presence of strong well-resolved maximums in a relatively narrow range of the IR spectrum, 2300–3000 cm^{-1}. Importantly, position of the $\nu(OH)(H_3O^+)$ band in the case of the complexes containing a free O–H bond in the H_3O^+ ion (H_3O^+–$2H_2O$ and H_3O^+–$5H_2O$) and in the complexes with all the O–H bonds forming the hydrogen bonds (H_3O^+–$3H_2O$ and H_3O^+–$6H_2O$) differed by ≈400 cm^{-1}; whereas the positions of the $\nu_s(OH)(H_3O^+)$ or $\nu_{as}(OH)(H_3O^+)$ bands in the spectra of the clusters of the same type but different nuclearity were different by only 10–20 cm^{-1}: H_3O^+–$2H_2O$, $\nu_s(OH)(H_3O^+)$ 2564(28.4) and $\nu_{as}(OH)(H_3O^+)$ 2337 (94.6) cm^{-1}; H_3O^+–$5H_2O$, $\nu_s(OH)(H_3O^+)$ 2588(60.5) and $\nu_{as}(OH)(H_3O^+)$ 2697(42.5) cm^{-1}; H_3O^+–$3H_2O$, $\nu_s(OH)(H_3O^+)$ 2966(11.1) and $\nu_{as}(OH)(H_3O^+)$ 2753 (70.3) cm^{-1}; H_3O^+–$6H_2O$, $\nu_s(OH)(H_3O^+)$ 2978(19.4) and $\nu_{as}(OH)(H_3O^+)$ 2741(40.3) cm^{-1}; H_3O^+–$3H_2O$, $\nu(OH)(H_3O^+)$ 2805(62.5) cm^{-1} (transfer of H^+ to H_2O) (0.44–1.56 Å); H_3O^+–$6H_2O$, $\nu_{as}(OH)(H_3O^+)$ 2662(40.1) cm^{-1}.

The spectra of the H_3O^+–nH_2O ($n \rightarrow 3$) clusters contained a band with maximums at 3100–3500 cm^{-1} evidencing about hydrogen bonding of the water molecules (with one of the O–H bonds being associated and the other one, terminal, remaining free). Hereafter the number of the coordination sphere of water molecule with respect to the hydroxonium ion is enumerated in the parentheses after the H_2O symbol. Those maximums appeared exclusively in the presence of water molecules connected via a hydrogen bond with one another. Evidently, the higher was the coordination sphere number, the closer was the $\nu_s(OH)(H_2O)$ frequency to that of $\nu(OH)$ of isolated water molecule: H_3O^+–$5H_2O$(I), $\nu_s(OH)(H_2O)$ 3494 (21.5) and 3374(21.8) cm^{-1}; H_3O^+–$6H_2O$(I), $\nu_s(OH)(H_2O)$ 3285(35.4), 3242(30.5), and 3171(23.6) cm^{-1}; H_3O^+–$6H_2O$(II), $\nu_s(OH)(H_2O)$ 3774(7.1), 3664(7.5), and 3637(7.0) cm^{-1}.

Another important indication of the presence of H_3O^+ ions [either isolated or part of the H_3O^+–nH_2O ($n \rightarrow 1$) complexes] was the presence of strong maximum at 890–1500 cm^{-1} assigned to the umbrella δ

(HOH) deformation. Frequency of that maximum increased with the growing cluster nuclearity: ν_{umbr} = 891 (n = 1), 1282 (n = 2), 1272 (n = 3), 1516 (n = 5), and 1442 (n = 6) cm^{-1}. The listed bands could be used for elucidation of the H_3O^+–nH_2O complex structure in the gas phase.

In the case of the $(H_3O^+–3H_2O)Cl^–$ complex, the frequency of symmetric stretching of water molecules were lower as compared to the other complexes. At the same time, deformational and asymmetric stretching vibrations of the chlorine-containing complex were similar to those of aqueous complexes of hydroxonium ion.

Noteworthily, the vibrational spectra were simulated at 298 K in the gas phase. It is therefore unclear whether the discussed trend of the umbrella vibration shift will be preserved at higher temperature. According to the experiment, vibrations of hydroxonium ion in the condensed phase were marginally different from the corresponding vibrations of water molecules [31].

To conclude, the study of hydroxonium ion and its small clusters with water molecules has revealed that the H_3O^+ ion is formed upon collision of water molecule and a proton via a barrier-free mechanism. Electron trapping with hydroxonium ion should be accompanied with the energy release. The H_3O^+–nH_2O ($n \leq 6$) small clusters are less stable and more hygroscopic as compared to water clusters. Therefore, the hydroxonium ion clusters can be viewed as a nucleus of the condensed phase with the hydroxonium ion being expelled to the surface rather than coordinated in the interior (since oxygen atom of H_3O^+ is not involved in the hydrogen bonding with water molecules). The presence of H_3O^+ in the aquatic clusters is reflected in the IR spectra in the appearance of well resolved relatively strong maximums at 2300–2900 cm^{-1}, absent in the spectra of water clusters and assigned to symmetric and asymmetric stretching of the hydrogen-bound O–H (H_3O^+) bonds. The maximums of $\nu_s(OH)(H_3O^+)$ are located at ≈400 cm^{-1} higher frequency in the cases of the clusters with all the three O–H bonds of H_3O^+ interacting with water molecules as compared to the clusters containing a single free (terminal) O–H bond in the hydroxonium ion. Symmetric deformation (umbrella) band at 900–1450 cm^{-1} is another important indication of the presence of H_3O^+ in its aquatic clusters; frequency of that vibration increases with the higher cluster nuclearity.

REFERENCES

1. Sazonov, B.I., *Solnechno-atmosfernye svyazi v teorii klimata i prognozakh pogody* (Solar-Atmospheric Bonds in Theory of Climate and Weather), 1972, p. 3.
2. Ardelyan, N.V., Bychkov, V.L., Bychkov, D.V., Denisiuk, S.V., Kosmachevskii, K.V., and Sablin, M.N., *9th Workshop Thermo-Chemical Processes in Plasma Aerodynamics*, St. Petersburg, 2012, p. 51.
3. Minaev, B.F., Lunnel, S., and Kobzev, G.I., *J. Quant. Chem*., 1994, vol. 50, p. 279. DOI: 10.1002/qua.560500405.
4. Minaev, B.F., Lunnel, S., and Kobzev, G.I., *J. Mol. Struct. (Theochem.),* 1993, vol. 284, p. 1. DOI: 10.1016/0166-1280(93)87173-B.
5. Kobzev, G.I. and Minaev, B.F., *Russ. J. Phys. Chem*., 2005, vol. 79, no. 1, p. 166.
6. Muldakhmetov, Z.M., Minaev, B.F., Kobzev, G.I., Nikolaev, V.D., and Nurtakanova, Zh.U., *Izv. Nats. Akad. Nauk Resp. Kazakhstan, Ser. Khim*., 2002, vol. 4, p. 12.
7. Kobzev, G.I., Urvaev, D.G., Davydov, K.S., and Zaika, Yu.V., *J. Struct. Chem*., 2012, vol. 53, no. 1, p. 12.
8. Kobzev, G.I., *Vest. Orenburg. Gos. Univ*., 2005, no. 1, p. 150.
9. Kobzev, G.I., *Vest. Orenburg. Gos. Univ*., 2005, no. 5, p. 102.
10. Kobzev, G.I., *Vest. Orenburg. Gos. Univ*., 2005, no. 6, p. 97.
11. Iuga, C., Alvarez-Idaboy, J.R., and Vivier-Bunge, A., *Chem. Phys. Lett.,* 2010, vol. 501, p. 11. DOI: 10.1016/j.cplett.2010.10.043.
12. Schriver, L., Barreau, C., and Schriver, A., *Chem. Phys*., 1990, vol. 140, p. 429. DOI: 10.1016/0301-0104(90)80009-M.
13. Cheng, Q., Evangelista, F.A., Simmonett, A.C., Yamaguchi, Y., and Schaefer, H.F., *J. Phys. Chem. (A)*, 2009, vol. 113, no. 49, p. 13779. DOI: 10.1021/jp907715a.
14. Goldman, N., Raymond, S.F., Leforestier, C., and Saykally, R.J., *J. Phys. Chem. (A)*, 2001, vol. 105, no. 3, p. 515. DOI:10.1021/jp003567a.
15. Kargovskii, A.V., *Computer Studies and Modeling*, 2009, vol. 1, no. 3, p. 321.
16. Yukhnevich, G.V., *Infrakrasnaya spektroskopiya vody* (Infrared Spectroscopy of Water), Moscow: Nauka, 1973, p. 211.
17. Kozlov, D.V., *Osnovy gidrofiziki* (Bases of Hydrophysics), Moscow: MGUP, 2004.
18. Radtsig, A.A. and Smirmov, M.M., *Spravochnik po atomnoi i molekulyarnoi fizike* (Handbook of Atomic and Molecular Physics). Moscow: Atomizdat, 1980.
19. Krasnov, K.S., *Molekuly i khimicheskaya svyaz'* (Molecules and Chemical Bond), Moscow: Vysshaya Shkola, 1984, p. 274.

20. Kryachko, E.S. and Zeegers-Huyskens, T., *J. Phys. Chem. (A)*, 2003, vol. 107, no. 38, p. 7546. DOI: 10.1021/jp022498s.
21. Edison, A.S., Markley, J.L., and Weinhold, F., *J. Phys. Chem*., 1995, vol. 99, no. 20, p. 8013. DOI: 10.1021/j100020a025.
22. Vener, M.V., Kong, S., Levina, A.A., and Shenderovich, I.G., *Acta Chim. Slov*., 2011, vol. 58, no. 20, p. 402.
23. Kaledin, M. and Wood, C.A., *J. Chem. Theor. Comput*., 2010, vol. 6, no. 8, p. 2525. DOI: 10.1021/ct100122s.
24. Jiang, J.C., Wang, Y.S., Chang, H.C., Lin, S.H., Lee, Y.T., Niedner-Schatteburg, G., and Chang, H.C., *J. Am. Chem. Soc*., 2000, vol. 122, p. 1398. DOI: 10.1021/ja990033i.
25. Cao, H.Z., Allavena, M., Tapia, O., and Evleth, E.M., *J. Phys. Chem*., 1985, vol. 89, no. 9, p. 1581. DOI: 10.1021/j100255a009.
26. Christie, R.A. and Jordan, K.D., *J. Phys. Chem. (A)*, 2001, vol. 105, no. 32, p. 7551. DOI: 10.1021/jp011241b.
27. Tang, J. and Oka, T., *J. Mol. Spectr*., 1999, vol. 196, no. 1, p. 120. DOI: 10.1006/jmsp.1999.7844.
28. Okumura, M., Yeh, L.I., Myers, J.D., and Lee, Y.T., *J. Phys. Chem*., 1990, vol. 94, no. 9, p. 3416. DOI: 10.1021/j100372a014.
29. Yeh, L.I., Okumura, M., Myers, J.D., Price, J.M., and Lee, Y.T., *J. Chem. Phys*., 1989, vol. 91, no. 12, p. 7319. DOI: 10.1063/ 1.457305.
30. Sobolewski, A.L. andf Domcke, W., *J. Phys. Chem*., 2002, vol. 106, no. 16, p. 4158. DOI: 10.1021/jp013835k.
31. Librovich, N.B., Maiorov, V.D., and Vinnik, M.I., *Russ. J. Struct. Chem*., 1973, vol. 14, no. 1, p. 14. DOI: 10.1007/BF00747464.
32. Asmis, K.R., Pivonka, N.L., Santambrogio, G., Brümmer, M., Kaposta, C., Neumark, D.M., and Wöste, L., *Science,* 2003, vol. 299, no. 5611, p. 1375. DOI: 10.1126/science.1081634.
33. Douberly, G.E., Walters, R.S., Cui, J., Jordan, K.D., and Duncan, M.A., *J. Phys. Chem*., 2010, vol. 114, no. 13, p. 4570. DOI: 10.1021/jp100778s.
34. Fridgen, T.D., McMahon, T.B., MacAleese, L., and Lemaire, J., Mait P., *J. Phys. Chem*., 2004, vol. 108, no. 42, p. 9008. DOI: 10.1021/jp040486w.
35. Headrick, J.M., Diken, E.G., Walters, R.S., Hammer, N.I., Christie, R.A., Cui, J., Myshakin, E.M., Duncan, M.A., Johnson, M.A., and Jordan, K.D., *Science*, 2005, vol. 308, no. 5729, p. 1765. DOI: 10.1126/science.1113094.
36. Begemann, M.H., Gudeman, C.S., Pfaff, J., and Saykally, R.J., *J. Phys. Rev. Lett*., 1983, vol. 51, no. 7, p. 554. DOI: 10.1103/PhysRevLett.51.554.
37. Grubele, M., Polak, M., and Saykally, R.J., *J. Chem. Phys.,* 1987, vol. 87, p. 3347. DOI: 10.1063/1.453029.
38. Librovich, N.B., Sakun, V.P., and Sokolov, N.D., *Russ. J. Theor. Exp. Chem*., 1979, vol. 14, no. 4, p. 393.
39. Davies, P.B., Hamilton, P.A., and Johnson, S.A., *J. Opt. Soc. Am. (B)*, 1985, vol. 2, no. 5, p. 794. DOI: 10.1364/JOSAB.2.000794.
40. Galashev, A.E. and Rakhmanova, O.R., *Khim. Fiz.*, 2011, vol. 30, no. 4, p. 3.
41. Koch, W. and Holthausen, M.C., *A Chemist`s Guide to Density Functional Theory*, 2001.
42. Smidt, M.W., Baldridge, K.K., Boatz, J.A., Elbert, S.T., Gordon, M.S., Jensen, J.H., Kozeki, S., Matsunaga, N., Nguyen, K.A., Su, S., Windus, T.L., Dupuis, M., and Montgomery, J.A., *J. Comput. Chem*., 1993, vol. 14, p. 1347. DOI: 10.1002/jcc.540141112.
43. Ferriso, C.C. and Hornig, D.F., J. *Chem. Phys*., 1955, vol. 23, p. 1464. DOI: 10.1063/1.1742330.
44. Paganetti, H., *Phys. Med. Biol*., 2009, vol. 54, p. 4399. DOI: 10.1088/0031-9155/54/14/004.
45. Huneycutt, A.J., Stickland, R.J., Hellberg, F., and Saykally, R.J., J. *Chem. Phys*., 2003, vol. 118, no. 3, p. 1221. DOI: 10.1063/ 1.1529177.
46. Bollinge,r J.C. and Faure, R., *Chem. Phys*. Lett., 1987, vol. 140, p. 579. DOI: 10.1016/0009-2614(87)80490-6.
47. Kiselev, A.V. and Lygin, V.I., *Infrakrasnye spektry poverkhnostnykh soedinenii* (Infrared Spectra of Surface Compounds), Moscow: Nauka, 1972.
48. Byakov, V.M. and Stepanov, S.V., *Usp. Fiz. Nauk UFN*, 2006, vol. 176, no. 5. 487 c.
49. Timokhin, V.M., Garmash, V.M., and Tedzhetov, V.A., *Sovremennye problemy nauki i obrazovaniya* (Modern Problems of Science and Education), 2013, no. 3. ISSN 2070-7428.
50. Kostrikin, A.V., Kuznetsova, R.V., Kosenkova, O.V., Merkulova, A.N., and Lin'ko, I.V., *Voprosy sovremennoi nauki i praktiki* (Questions of Modern Science and Practice), Univ. im. V.I. Vernadskogo, 2007, no. 2(8), p. 181.
51. Zaitsev, B.E., *Spektroskopicheskie metody v neorganicheskoi khimii* (Spectroscopic Methods in Inorganic Chemistry), Moscow: RUDN, 1974, part 1.
52. Sovoie, R. and Giguere, P.A., *J. Chem. Phys*., 1964, vol. 41, p. 2698. DOI: 10.1063/1.1726340.
53. Giguere, P.A. and Madec, C., *Chem. Phys*. *Lett.*, 1976, vol. 37, p. 569. DOI: 10.1016/0009-2614(76)85040-3.
54. Glushko, V.P., *Termodinamicheskie svoistva individual'nykh veshchestv* (Thermodynamic Properties of Individual Substances), Moscow: Nauka, 1978, vol. 1, book 1.
55. Krasnova, K.S., *Molekulyarnye postoyannye neorganicheskikh soedinenii* (Molecular Constants of Inorganic Compounds), Leningrad: Khimiya, 1979.
56. Morozov, V.P., Dergachev, M.P., and Lasunin, M.V., *Russ. J. Struct. Chem*., vol. 44, no. 6, p. 1004. DOI: 10.1023/B:JORY.0000034802.51499.ff.
57. Scott, A.P. and Radom, L., *J. Phys. Chem*., 1996, vol. 100, no. 41, p. 16502. DOI: 10.1021/jp960976r.